Current Journal of Applied Science and Technology

36(3): 1-20, 2019; Article no.CJAST.49572
ISSN: 2457-1024
(Past name: British Journal of Applied Science & Technology, Past ISSN: 2231-0843, NLM ID: 101664541)

Geochemical and Petrographical Evolution of the Weathering Mantle Derived from Basalt in Bangam Locality (West-Cameroon): Implication in the Bauxitisation Process

Taylor Moise Sojien[1], Estelle Lionelle Tamto Mamdem[2], Armand Sylvain Ludovic Wouatong[1*] and Dieudonne Lucien Bitom Oyono[3]

[1]Department of Earth Sciences, Faculty of Sciences, University of Dschang, P.O.Box 67, Dschang, Cameroon.
[2]Department of Earth Sciences, Faculty of Sciences, University of Ngaoundéré, P.O.Box 454, Ngaoundéré, Cameroon.
[3]Department of Earth Sciences, Faculty of Sciences, University of Yaoundé 1, P.O.Box 812, Yaoundé, Cameroon.

Authors' contributions

This work was carried out in collaboration among all authors. Authors TMS, ELTM and ASLW designed the study, wrote the protocol and wrote the first draft of the manuscript. Authors ELTM, ASLW and DLBO managed the analyses of the study. Authors TMS and ELTM managed the literature searches. All authors read and approved the final manuscript.

Article Information

DOI: 10.9734/CJAST/2019/v36i330231
Editor(s):
(1) Dr. Pavel K. Kepezhinskas, PNK GeoScience, Tampa, Florida, USA.
Reviewers:
(1) Snehadri Ota, Institute of Physics, India.
(2) Jianhui Yang, Henan Polytechnic University, China.
(3) Rosario García Giménez, UAM, Spain.
Complete Peer review History: http://www.sdiarticle3.com/review-history/49572

Original Research Article

Received 05 April 2019
Accepted 10 June 2019
Published 05 July 2019

ABSTRACT

A petrographical and geochemistry study of weathering mantle derived from the basaltic parent rock (plagioclase, olivine, pyroxene, zircon) has been conducted in the locality of Bangam (West-Cameroon). The weathered profile shows a vertical lithology succession of weathered parent rock, isalteritic clayed domain and superficial duricrust (alloterite). The weathering of basalt started by the formation of "pain d'epices" structure rich in gibbsite, metahalloysite, kaolinite. The geochemistry

**Corresponding author: E-mail: aslwouat@yahoo.com;*

analysis of major elements indicate that SiO_2 (46% -1.33%), K_2O (0.84% - 0.01%), Na_2O (3.6% - 0.01%), MnO (0.3% - 0.04%), P_2O_5 (1.9% - 0.38%) and CaO (5% -0.02%) decrease from the bottom to the surface, however TiO_2 (2.3% - 4.08%) remain constant, Fe_2O_3 (24.2% - 24,6%) and Al_2O_3 (14.5% - 45.2%) increase. The different weathering index such as, chemical index of alteration (55% - 99%), index of lateritization (41% - 103.5%) and Ruxton Ratio (0.12 - 3.21) just indicate an evolution of parent rock dominated by an alumina and iron phases under a control of hydrolysis phenomenon as bisialitisation, monosiallitisation and allitisation with the formation of minerals smectites group, kaolinite group gibbsite and iron oxides group. The fractionation patterns of rare earth elements (REE) show a positive and negative anomaly in Cerium and other rare earth elements, one more, the correlation between major, trace and REE prove a link of different pedological horizons developed on the basalt in redox condition.

Keywords: Basalt; mineral; geochemistry; evolution; bauxite.

1. INTRODUCTION

The locality of Bangam and its surroundings are located in zone 32N 636000.651000 and 597500.587000 (Fig. 1). It is subjected to a pseudo-equatorial climate [1] with four seasons [2]. The wet savannah is the type of vegetation encountered in Bangam [3]. On the geological plan, our study area is an integral part of the Cameroon volcanic line [4] which crosses the Western part of the Cameroonian territory. The formations of the metamorphic basement are represented by mylonitized gneiss with gray or dark color with difficulty showing an alternation of millimetric to centimetric beds composed of quartz, feldspar, garnet-kyanite-biotite or garnet-kyanite-biotite. These rocks were deformed during two tectonic phases [5]. The gneiss with muscovite (orthogneiss) and biotite are also observed, the foliations are very weakly differentiated with ptygmatic folds. The plutonic formations are mostly represented by leucocratic granites with a porphyritic granular texture that belongs to the Batié plutonic complex [6] outcropping as a dome syn to late kinematic with a tertiary age [7]. The volcanic rocks found here are aphyric and porphyric basalts known as “basalte de plateau” [8] formed during the second volcanic phase of quaternary [9] with following minerals observed: plagioclases of bytownite-labrador type, olivine and pyroxene. In most cases, these plutonic, volcanic and metamorphic rocks can be transformed in the meteoritic condition in tropical environment to form bauxites. The bauxites duricrust belongs to the family of lateritic soils that occupy around 33% of intertropical [10]. They are formed under a dry contrast tropical climate or wet equatorial climate [11-15]. In Cameroon, many authors have studied the petrology of lateritic duricrust in Adamaoua [16], in the West [17] and in the equatorial region [18-22]. The study of bauxites in Bangam and its environs have been subjected to many scientist research’s [23-25] on the characterization and cartography of the different bauxites facies, in addition, many geological studies have been done in our research zone [7]. In a context where the research on bauxites is booming in Cameroon, the previous work on the Bangam Bauxites done by [8,9] and [26] were incomplete and theirs genesis remain unknown, however, no work in date has concentrated on the parent rock evolution, the genesis of bauxites and the transformation of ore body in the alteration mantle. Consequently, the purpose of this work is to identify the exact nature of parent rock and address or show the petrograpical and geochemistry evolution of alteration coat developed during geological times.

2. MATERIALS AND METHODS

The research has been done both on the field and in the laboratory.

Firstly, the work on the field consisted of digging trials pits in the form of a toposequence (Fig. 2) in the study area and then, collecting samples immediately from the bottom to the surface following the morphological variations. A morphopedological description was made according to the protocol proposed by [27], which consisted of a detailed study of the soil horizons. The samples collected in the alteration coat were sent to the laboratory.

Secondly, in addition to field studies, petrographic analyze were performed on indurated rocks at the Nkolbisson Geology Laboratory of the University of Yaoundé I. Chemical analyses were done on the duricrust and weathered rock at ALS in South-Africa (Alex Steward Laboratory) for major, trace and rare earth elements. Chemical elements identification

and quantification were performed by the X-ray fluorescence spectrometry method (ME.ICP 06, ME MS81, OA-GRA05). Spectrometer mass contents are reported as a percentage of oxides (%) for major elements and as part per million (ppm) for trace and rare earth elements.

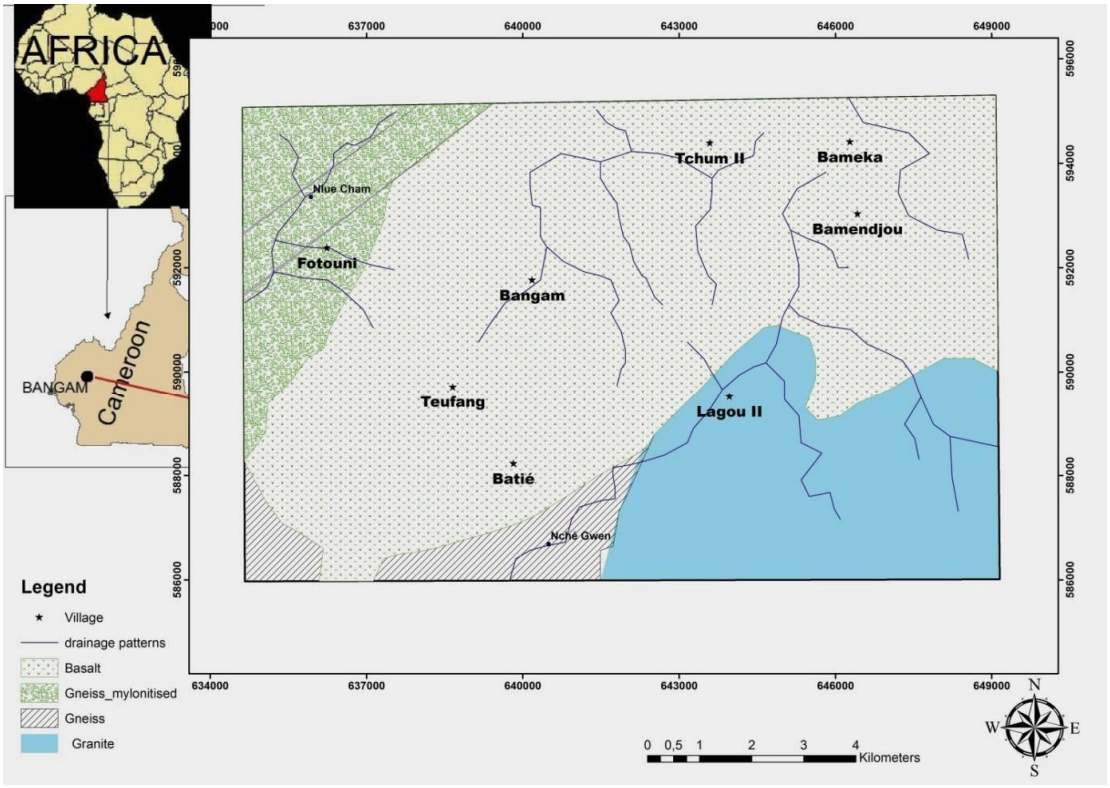

Fig. 1. Location and geological map of Bangam in the West-Cameroon region

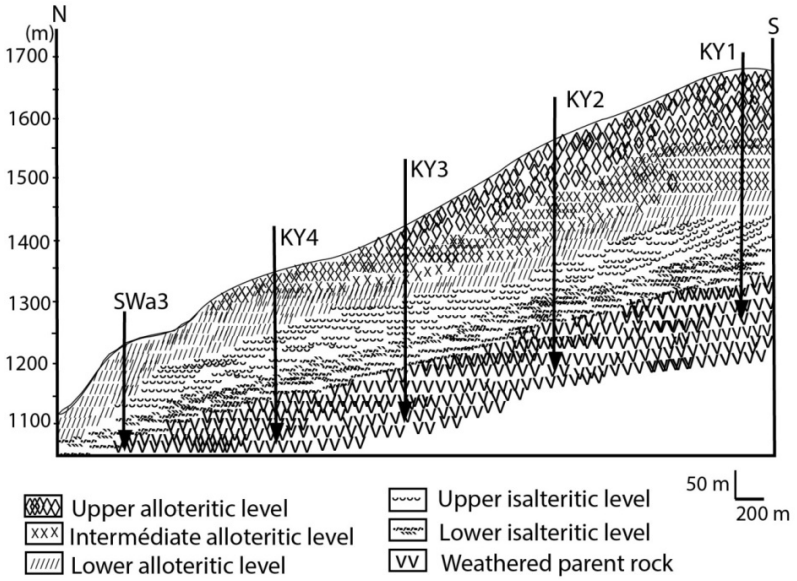

Fig. 2. Toposequence on the flank of Kong-Yeni plateau (Bangam)

In addition, three soil weathering index were inferred from the major element data. They are: the chemical index of alteration (CIA = $[Al_2O_3/(Al_2O_3 + CaO + Na_2O)]x100$ proposed by [28], the molar ratio SiO_2/Al_2O_3 of [29] and the index of lateritization $[(Al_2O_3+Fe_2O_3)/(SiO_2+ Al_2O_3+Fe_2O_3)]$ of [30]. The geochemical balances to assess the gain and loss of materials were done according the equation Ψ (%) =100x [Element (%) $_{horizon}$/Element (%) $_{rock}$ -1] proposed by [31]. A statistical study based on the correlation coefficient of Spearman has been used to treat the different results and the correlation matrix was calculated by Excel software. The REE concentrations were normalized relative to basalt and chondrite [32] to facilitate the comparison of the REE patterns between weathering materials. The (La/Yb)N ratios were calculated to indicate the degree of light rare earth element(LREE) and heavy rare element(HREE) fractionation. Europium (Eu) and Cerium (Ce) anomalies were respectively estimated by comparing the measured concentration of Eu with an expected concentration (Eu*) obtained by interpolation between the normalized values of Sm and Gd and by comparing the measured concentration of Ce with an expected concentration (Ce*) obtained by interpolation between the normalized values of La and Pr as proposed by [33], the results obtained from the above analyses were carried out to understand the behaviour of chemical elements along the profile.

3. RESULTS

In the Bangam locality, five alteration profiles KY1, KY2, KY3, KY4 and SWa3 (Fig. 2) have been studied according to the toposequence oriented N-S on the southern flank of the Kong-yeni plateau. The alteration profile KY1 has been chosen and illustrated (Fig. 3). It has a depth of 19 m and has three levels of classification and subdivided by pedological horizon from the top of the profile to the parent rock. The geographic coordinates is UTM 32N, 589080 and 640620, at 1680 m of altitude.

3.1 Overview of Weathering Mantle of KY1

A KY1 weathering mantle has 19 m of depth and is organized in A_0, B_{E1}, B_{E2}, B_{E3}, B_{E4}, B_I, C_1 and C_2 horizons.

The 0 cm-10 cm depth consists of the organic horizon A_0. It is very thin, well leached by a bioturbation phenomenon. The presence of vegetal roots and burrow animals are also noticed in this horizon. The lateritization process is weakly developed and relatively to the high concentration of black soil (7.5G.2/1.5), the transition with the lower eluvial horizon is undulated.

The 10 cm-300 cm depth consist of the BE1 is characterized by a weak presence of very fine grain of materials such as reddish-brown clays (10R.3/3), the high presence of consolidated blocs of duricrust with metric and centimetric sizes. The blocs and boulders are bounded to each other by a fine clay particle. The nodular, massive, pisolitic facies are strongly represented along the profile and their size decreases considerably from the top to the bottom of this horizon. The color also varies according to the facies and the transition is gradual with the lower horizon by the size of the blocks.

The 300 cm-400 cm depth consist of the B_{E2} horizon made up with some scattered nodules of reddish (5R.4/9.5), color of centimetric size. The boulder found here has a characteristic of pisolitic facies and with irregular sharp. The leaching phenomenon is total, with around 80% of blocs having pore full of some mottled clays particles. Mottled clays are sometimes incorporated between blocs and boulders. The brown reddish color disappears progressively and relatively to the brown grey color.

The 400 cm-1000 cm depth comprises different metric blocs and boulders, separated by a medium grain of clays. The red color is dominated (10R.3/3) by other color that can be observed such as red brown (7.5R.4.5/10). We can also observe a heterogeneity of facies scattered with nodules and pisoliths. The transition with the lower horizon is gradual and the sizes of boulders and blocs decrease progressively toward the bottom.

The 1000 cm – 1400 cm depth consist of the B_{E4} horizon which is characterized by a general dismantling of boulders and we observe the degree of humectation is higher than the upper zone of this profile. The centimetric blocs with polyhedric sharps of duricrust and brown-yellowish clays (10YR.7.5/11) are highly represented. This domain marks the transition between the leaching zone and accumulation zone.

The 1400 cm-1500 cm depth is B_I horizon also called illuviation horizon. It's characterized by

very fine grain materials of clay particles, whereby the structure of weathered products haven't been preserved during alteration process. In some places within this horizon, weakly consolidated clays, occur which are relics of the parent rock which are no longer in existence and there is gradual appearance of spotted clays. A little stratification of alumina silicate and ferromagnesian minerals is clearly observed in this part of the profile. Nodule cannot be identified in the clays, however, the color change gradually from greyish clays to whitish clays.

The 1500 cm - 1650 cm depth is the C_1 horizon or upper isaltérite, a relic of parent rock also called structure in "pain d'épice" are clearly identified and indicate the transition between B_I horizon and C horizon; the limit is progressive toward the bottom with the appearance of greyish color (7.5GY.4.5/2) and coarse grains particles.

The depth from 1650 cm – 1850 cm is the C_2 is also called lower isalterite. The duricrust is brittle between fingers, has an irregular sharp and mainly sandwiched between clays particles. The color of this horizon is dark-pinkish (5RP.4/12), the "pain épice" structures observed in other parts of this horizon can indicate the nature of parent rock. The transition with the next horizon (C_1) is gradually.

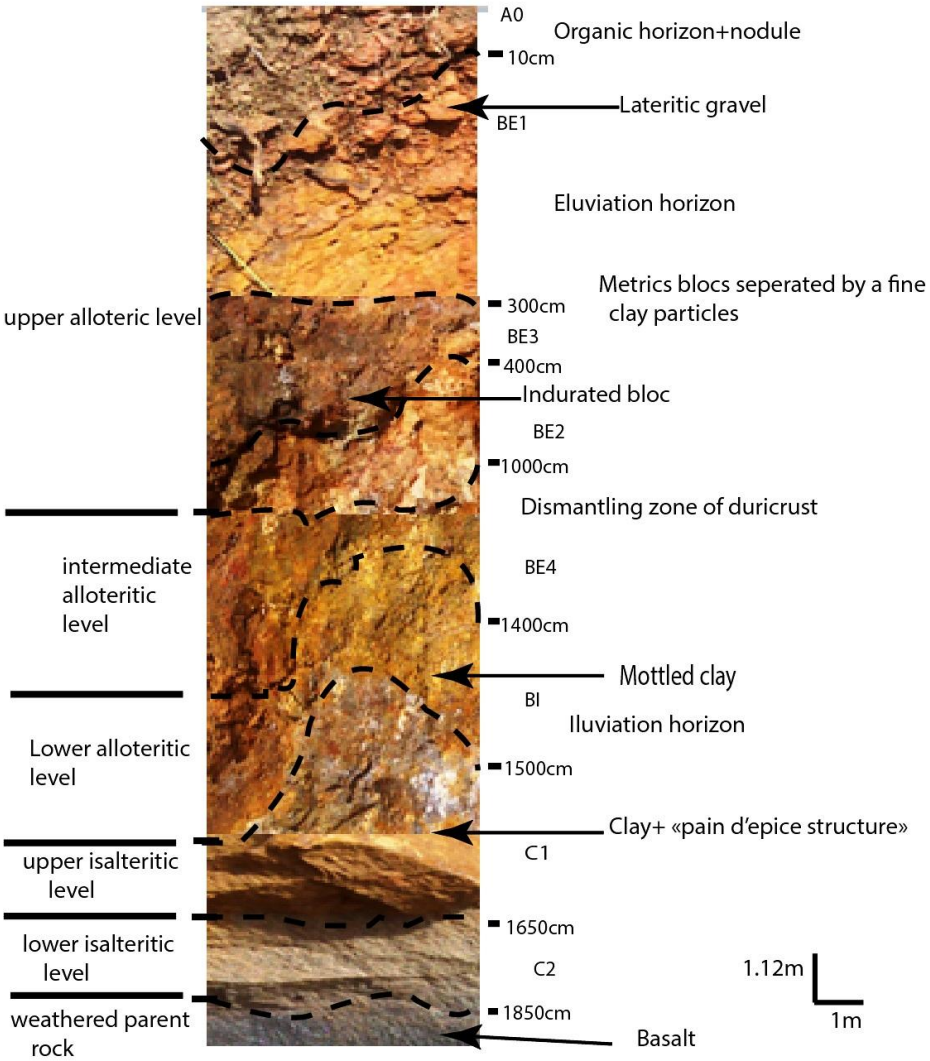

Fig. 3. Overview of weathering mantle of KY1 profile

At the depth of 1850 cm – 1900 cm, the structure of parent rock is partially conserved and made up of a coarse saprolite. The weathering materials are constituted by compact clays with a greyish color (7.5GY.4.5/2). The parent rock presents a weathered cortex that is well developed and a fresh part grey dark with microlitic texture known as basalt. The following description shows that, the alteration coat derived from the basalt rocks under the geochemical and mineralogical transformation.

3.2 Petrographical of Sample Collected in the Weathering Mantle

A petrographical study of the sample collected in the weathering zone on thin sections indicates primary minerals such as plagioclases, pyroxenes, olivine and magnetite. Some secondary minerals as kaolinite, hematite, goethite and gibbsite are also observed.

3.2.1 Olivine

Olivine is a ferromagnesian mineral observed in a thin section with an argilosepic matrix (Fig. 4a), it has a brownish color with many cracks that shows a starting zone of weathering. Pseudomorphosis or iddingsitisation of olivine is proof by the presence of a little fragmented minerals and the gradually domination of iron oxides such as goethite and hematite. The olivine has around 2 mm of size in a thin section and is characterized by a very low pleochroism.

3.2.2 Pyroxenes

The pyroxenes (Fig. 4b) are easily observable with a size of 2.5 mm and their basal section which presents the two suborthogonals cleavages plans (110). The cleavages zones might contain a whitish and reddish mineral in natural light. It's mostly associated with clayed minerals characterized by a vosepic structure, the replacement process is gradually observed by the presence of alumina silicate such as kaolinite.

3.2.3 Plagioclases

In thin sections, the plagioclases are a fresh mineral in some sections, and weakly weathered in others (Fig. 4d). It's more ever in association with zircon inclusions with an elongated form, millimeters sizes and preferential orientation. The minerals are also easily identified by their multiple macles. Their size is significantly reduced where the phenomenon of argiliplasmation takes place. We found plagioclases mostly in association with opaque oxides, hydroxides and other alumina silicates and without preferential orientation (insepic).

3.2.4 Hematite / Goethite

Hematite and goethite are represented in thin sections (Fig. 4c) by a reddish and brownish red zone. They are characterized by a low pleochroism and two forms of structural orientation, massepic in some sections and insepic in others. They are always found in association between the fissures of primary minerals and which sometimes serve as ferruginous bridges between gibbsite and kaolinite. Hematite and goethite are mostly represented in pisolitic and pseudobréccia facies. Hematite is mostly associated with goethite and appears commonly between primary minerals.

3.2.5 Magnetite

Magnetite appears in thin sections by an irregular shape (Fig. 4b), they have a very dark color and no pleochroism .It's mostly associated with others Fe-oxides minerals, Al-oxides and in inclusion with the remains of primary minerals.

3.2.6 Gibbsite

The gibbsite mineral is always colorless in thin sections (Fig. 4b) and there isn't any color of iron mineral [34] and whitish in some sections [35]. It presents as cutaneous and appears without orientation (insepic) and always in association with plagioclases and others silicate minerals. Gibbsite is mainly found in the transmineral crack and takes place gradually to the detriment of iron oxides.

3.2.7 Kaolinite

This alumina mineral is strongly observed in a thin section of grey-bluish to whitish color (Fig. 4b). It's mostly associated with gibbsite and other iron clayed minerals; kaolinite progressively takes the place of some unidentified primary minerals. It is observed here as the grey transition zone of kaolinite which marks the transition from kaolinite to gibbsite. The genesis of kaolinite starts more often in the cracks of primary minerals such as plagioclases and pyroxenes [36].

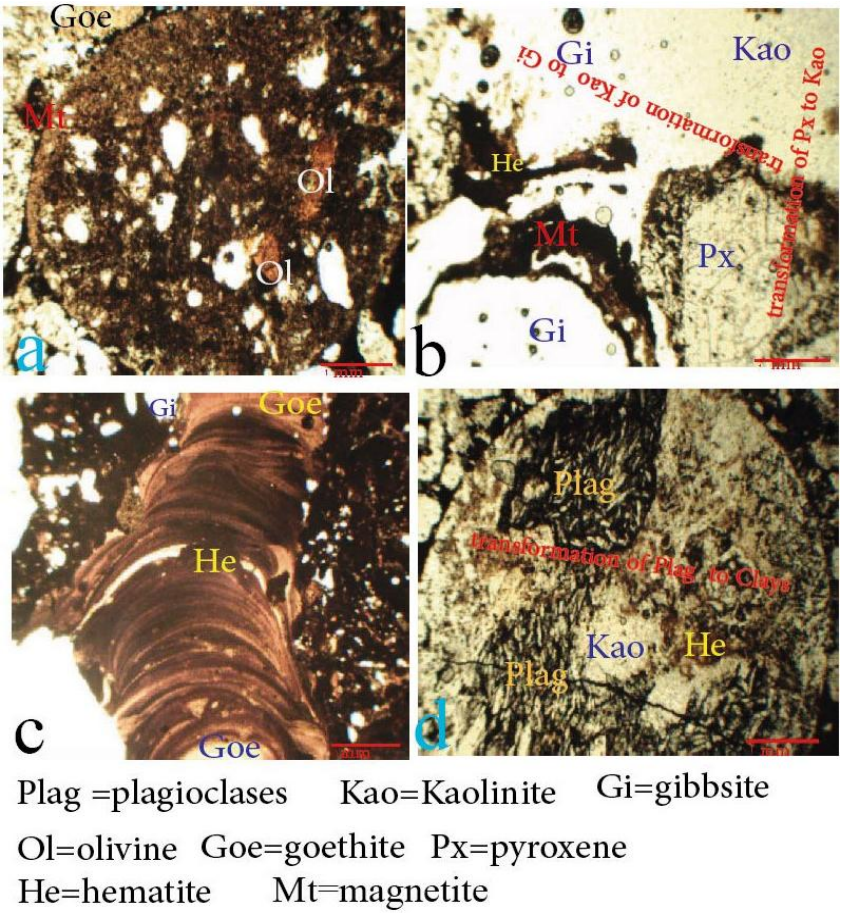

Fig. 4. Petrographical observation in thin section

3.3 Geochemical Mobilization and Redistribution in the Weathering Mantle

3.3.1 Major and trace elements contents

The major and trace element contents are given in Table 1.

According to the Table 1 and Fig. 5, we observe that silica contents decrease significantly from weathered parent rock to the red brown alloterite of the B horizon (SiO_2: 46 to 1.33%). Inversely, aluminum (Al_2O_3: 14.35 to 45.2%) and iron (Fe_2O_3: 24.5 to 38.5%) contents increase relatively toward the surface. Calcium (CaO: 5.0 to 0.02%), sodium (Na_2O: 3.6 to 0.0%), potassium (K_2O: 0.6 to 0.0%), magnesium (MgO: 3.1 to 0.07%) are almost completely leached in the weathering mantle. However, titanium (TiO_2: 2.3 to 4.08%) and manganese (MnO: 0.3 to 0.04%) remain constant from the weathered rock to the red brown saprolite. Concerning trace elements, we can observe in Fig. 5 that Cs (0.22-0.01ppm) and Rb (19.8 - 0.3ppm) decrease from the bottom to the surface , Ga (26.2 - 51.1ppm), Nd (34 -74ppm) and Th (3.69 - 11.85ppm) are slightly constant, however U (0.82 - 4.38pp), Sn (3 - 4ppm), Sr (474 - 103ppm), V(232 - 337ppm),Ta (2.2 - 9.4ppm) and Ba (337 - 144ppm) have a zig-zag evolution.

3.3.2 Geochemical evolution of KY1 profile by triangular diagrams and weathering index

Due to the normalization of the percentage oxides in millication in which the sum of the three elements studied as total value corresponds to the 100 % content, two triangular diagrams $CaO+Na_2O$-Al_2O_3-K_2O, SiO_2-Al_2O_3-Fe_2O_3 and molar ratio SiO_2/Al_2O_3 have been realized according the Table 3. The analysis of the first diagram or diagram of chemical index of

alteration (CIA) allow to trace the intensity of alteration in particular, the evolution of feldspar and primary minerals by comparing the departure of Ca, Na, K with the evolution of Al (Fig. 8a). The chemical index of alteration related to weathering intensity, decreases very slightly from the bottom to the surface (see Table 3). We observe that Ca, Na, K is mostly leached (impoverishment) in the profile and the major samples are migrated toward the alumina pole (enrichment).In addition, chemical evolution can be also characterized by lateritization process. In this case, the diagram (Fig. 8b) shows that, the parent rock of Bangam profile is not a fresh rock, however, dominated by the kaolinisation at the bottom and the strong lateritization on the surface of profile. The IOL values (see Table 3) that is controlled by iron indicate a both evolution of an alumina phase and iron phase during the lateritization process. The molar ratio SiO_2/Al_2O_3 or Ruxton Ratio clearly shows the normal evolution of weathering mantle (Table 4). At the bottom of profile or lower isalterite we observe the values between 3.21-3.16, 1.25-1.07 in the lower allotérite and 0.99-0.15 in the upper allotérite.

3.3.3 Major and trace elements balance

The balance calculation of chemical elements of the Bangam alteration profile shows a group of accumulated elements such as Al (21,5%),Ti (2,17%), U (434ppm), Ta (327ppm),Th (260ppm), Zr (174ppm), Ga (120ppm) and Nb (178ppm). The group of exported elements such as Si (-97.1%), K (-100%), Na (-88%), Mn (-90%), Ba (-62ppm), Cs (-100ppm) and Rb (-100ppm). These elements are strongly leached

Table 1. Geochemistry of major and trace elements

Horizon		**PR**	**C1**	**C2**	**Bl**	**Bl**	**BE**	**BE**	**BE**	**BE**	**BE**
Sample		**P1**	**P2**	**P3**	**P4**	**P5**	**P6**	**P7**	**P8**	**P9**	**P10**
Color		**G**	**Gy**	**Gy**	**Wp**	**Rb**	**R**	**Br**	**Br**	**Br**	**Wy**
Depth(m)		**19**	**18.5**	**17**	**15**	**11.5**	**8**	**6**	**2**	**1**	**0.3**
lithology		**B**	**WB**	**WB**	**Fs**	**Sc**	**Nd**	**Pd**	**Md**	**Md**	**Md**
Oxides (%)	**DL**										
SiO_2	0.01	46	42.5	44.9	29.3	21.2	28.2	29.9	6.3	4.5	1.3
Al_2O_3	0.01	14.3	17.2	14.2	23.5	40.7	35.7	30.2	35.2	30.2	45.2
Fe_2O_3	0.01	24.5	25.6	21.3	25.4	10.9	38.5	18.1	32.6	38.5	24.6
CaO	0.01	5	2	8.2	0.0	00	0.0	0	0	0	0
MgO	0.01	3.1	2.1	4.2	0.1	0.1	0	0.1	0.1	0	0
Na_2O	0.01	0.9	3.6	2.8	0	0	0	0	0.	0	0.
K_2O	0.01	0.6	0.8	0.4	0	0	0	0	0	0.	0.
TiO_2	0.01	2.3	7.3	5	7.1	5.5	4.5	5	5	4	4
MnO	0.01	0.3	0	0.2	0.1	0	0	0	0	0	0
LOI		4.1	4.2	3,2	13.9	17	17.2	14.5	20.2	19.9	25.5
Total		103.6	104.2	103.2	99.9	99.7	99.5	99.3	100.1	98	101.2
Trace elements (ppm)											
Ba	0.5	337	297	287	14.5	402	126	335	125	121	144.5
Cs	0.01	0.2	026	0.12	0.01	0.0	0.0	0.03	0.0	0.0	0.0
Ga	0.1	26.2	25.4	36.5	42	59.2	55.5	41.5	57.9	48.6	51.1
Nb	0.2	34.2	25.2	62.3	41.7	59.9	35.6	43.3	95.4	49	74.5
Rb	0.2	19.8	17.8	21.3	0.6	0,6	0.32	0.6	0.5	0.3	0.3
Sn	1	3	3.5	7	3	4	2	3	6	5	4
Sr	0.1	474	464	424	6	418	145	273	91.8	79.7	103
Th	0.05	3.6	4	8.2	4.2	7.9	5	6.3	13.3	7.5	118
U	0.05	0.8	0.9	0.8	2.2	2.7	4.2	1.9	3.1	3.8	4.3
Zr	2	251	623	297	340	490	332	345	689	391	543
V	5	232	145	330	580	603	652	482	638	603	337
Ta	1	2.2	3.9	3.2	2.5	3.4	2	2.6	5.2	2.5	9.4

G=grey; Gw=whitish grey; Gy=Yellowish grey; Wy=Yellowish-white; Wp=Whitish-pink; Rb=red brown; R=redish; Br=brown red; Md=massive duricrust; Pd=Pisolitic duricrust, Nd=nodular duricrust; B=basalt; Wb=weathered basalt; Cs=coarse saprolite; Fs=Fine saprolite; Sc=Spoted clays; DL=detection limit. LOI= loss of ignition. PR= parent rock

of the weathered parent rock. The group of zig-zag elements is represented by Fe, Ca, Cr and Sn, which show an enrichment in the isalterite and sometimes are evacuated in the duricrust or upper allotérite. Ba (402 to 14.5ppm) Rb (19.8 to 0.3 ppm), Sr (474 to 103ppm) and Cs (0.22 to 0.00ppm) are the traces elements in this weathering mantle that decrease, inversely, V (232 to 638ppm), Zr (251 to 689 ppm), followed by Th (3.69 to 11.85 ppm), U (0.82 to 4.38 ppm), Ga (26.2 to 51 ppm) and Sn (3 to 4 ppm) are increasing along the profile.. In sum, these elements can be classified according to their increasing mobility as follow: K > Na >Si> Mn> Ca> Ba> Cs > W> Cr> Mg> P> Fe> Rb> Sn> Sr> Al> Ti> Ta > Th> Zr> U.

3.3.4 Geochemical correlation of Bangam profile

During the bauxitisation process, the chemical elements are redistributed along the profile and are linked by some affinities which permit to correlate them. In this case of the alteration of Bangam profile, we can distinguish positive and negative correlations. Firstly SiO_2 is highly correlated with Sr (0.7), Rb (0.79) and Cs (0.9), CaO with Rb (0.97) and Sr (0.71), Al_2O_3 with Cr (0.725) and Ga (0.891), Na_2O with Cs (0.77), Rb (0.81) Sr (0.8), K_2O with Cs (0.96) and Rb (0.91), La with Pr and La with Ce respectively of 0.95 and 0.93, we can also observed a weak correlation between Al_2O_3 and SiO_2 (0.58), samples are scattered around the graph on contrary of these REE as La/Pr (0.95), La/Ce (0.93) and trace elements Sr/Ba (0.85) where samples are nearly concentrated around the graph (Fig. 6).

Secondly, MnO is negatively correlated with U (-0.9) and V (-0.8), MgO with U (-0.81) and V (-0.77), Na_2O with Cr (-0.7), Ga (- 0.84), U (-0.8) and V (-0.8), CaO and U (-0.74), K_2O with U (-0.79) and V (-0.94), Al_2O_3 with Rb (-0.84) and SiO_2 (-0.58) , SiO_2 with Cr (-0.8) and U (-0.86).

Table 2. Rare earth element and fractionation

Horizon		**PR**	**C1**	**C2**	**Bl**	**Bl**	**BE**	**BE**	**BE**	**BE**	**BE**
Sample		**P1**	**P2**	**P3**	**P5**	**P7**	**P8**	**P9**	**P11**	**P12**	**P13**
Color		**G**	**Gy**	**Gy**	**Wp**	**Rb**	**R**	**Br**	**Br**	**Br**	**Wy**
Depth(m)		**19**	**18.5**	**17**	**15**	**11.5**	**8**	**6**	**2**	**1**	**0.3**
lithology		**B**	**WB**	**WB**	**Fs**	**Sc**	**Nd**	**Pd**	**Md**	**Md**	**Md**
RRE(ppm)	**Dl**										
La	0.5	40.5	100	41	13.6	100.5	121	278	79	89.8	65.1
Ce	0.5	87.7	83.7	86.3	27.8	186	171	552	133.5	162.5	123.5
Pr	0.03	12.3	13	14.2	3.1	22.7	23.6	69.4	18.1	19.6	15.2
Nd	0.1	55.7	18	24	11.9	90.9	75.6	253	75.2	75.7	61.1
Sm	0.03	13.2	12.5	11.5	2.5	20.2	23	50.5	15.5	15.7	13.0
Eu	0.03	3.4	1,3	2.37	0.6	4.9	4	12.1	3.4	3.3	3.5
Gd	0.05	12.0	13	11	1.7	17.7	13.5	30.2	12.4	12.1	11
Tb	0.01	1.8	1.5	1.6	0.3	2.7	1.6	4.0	1.6	1.7	1.5
Dy	0.05	9.0	11	5	1.8	18.1	8.2	18.8	8.4	8.7	7.1
Ho	0.01	1.6	2.4	2	0.35	4.2	1.3	2.4	1.2	1.2	1.0
Er	0.03	4.3	3.3	4.7	1.04	10.8	2.6	4.8	2.8	2.6	2.3
Tm	0.01	0.5	0.3	0.4	0.1	0.9	0.3	0.4	0.3	0.3	0.2
Yb	0.03	3	2.3	4.3	1.2	3.5	1.7	2.3	2.1	1.7	1.3
Lu	0.01	0.4	0.2	0.4	0.1	0.35	0.2	0.2	0.3	0.2	0.1
Hf	0.2	6.5	15	17.2	8.4	11.6	8.2	8.6	15.9	9.4	12.8
Y	0.5	41	36	45	6.6	103.5	29.9	35	23.9	21.5	19.5
RRE index											
ΣREE		245.9	262.7	208.9	66.5	483.8	447.8	1278.3	354.3	395.5	306.3
LREE/HREE		4.2	5.7	4.7	6.4	5.2	10.6	14.1	7.7	9.4	8.1
(La/Yb)N		1	3.1	0.7	0.7	2.0	5.1	8.8	2.7	3.7	3.5
Eu/Eu*		1	0.3	0.7	1.0	0.9	0.8	1.1	0.9	0.8	1.0
Ce/Ce*		1	0.5	0.9	1.0	0.9	0.8	1.0	0.9	0.9	1

G=grey; Gw=whitish grey; Gy=Yellowish grey; Wy=Yellowish-white; Wp=Whitish-pink; Rb=red brown; R=redish; Br=brown red; Md=massive duricrust; Pd=Pisolitic duricrust, Nd=nodular. Dl=detection limit

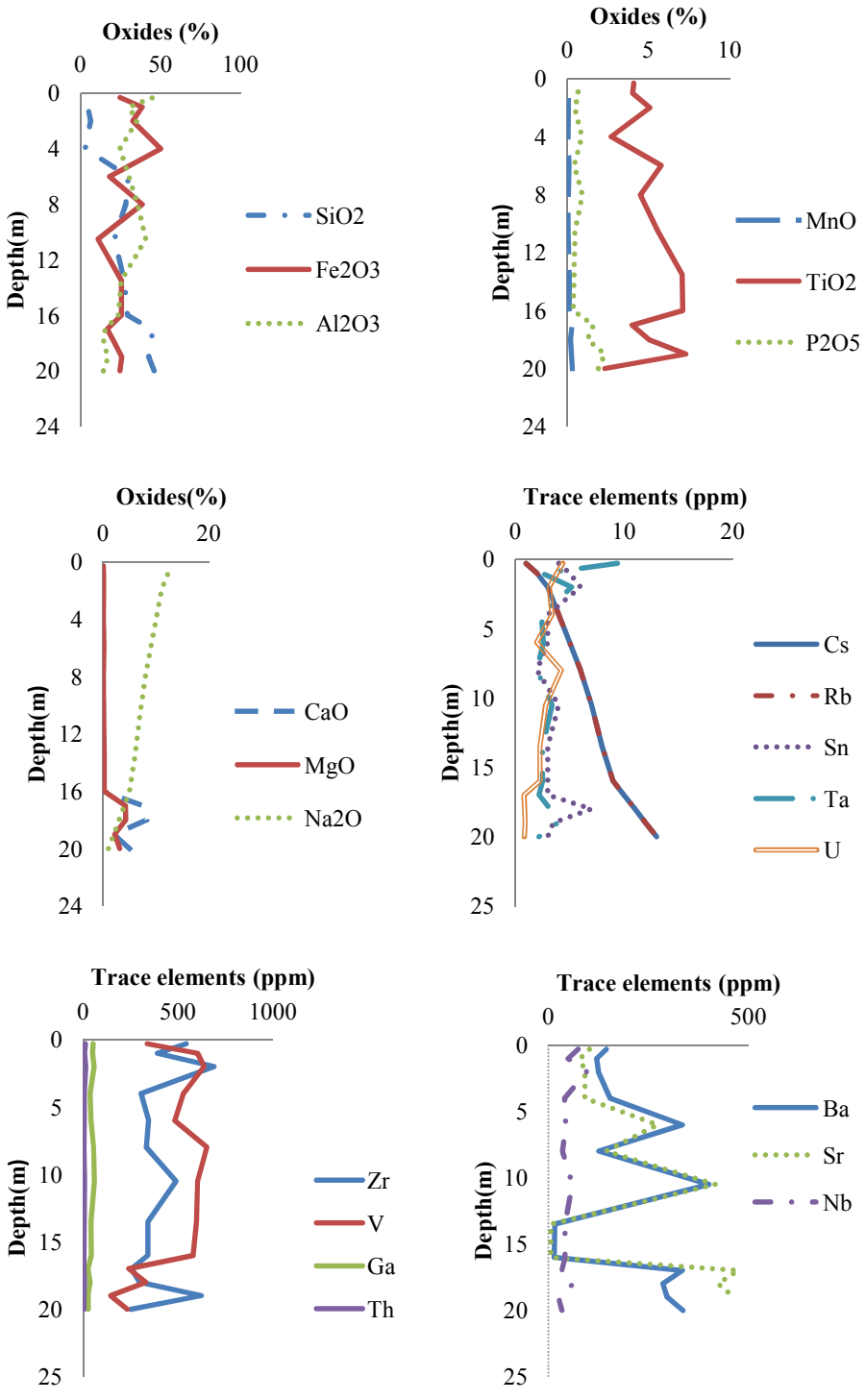

Fig. 5. Chemical distribution of major elements (wt% oxide) and trace (ppm) elements in the lateritic profile

Table 3. Chemicals index of alteration of KY1 profile

	Samples collected along of KY1 profile									
Chemicals index	**P1**	**P2**	**P3**	**P4**	**P5**	**P6**	**P7**	**P8**	**P9**	**P10**
CIA (%)	55	57	68	72	99	99	99	99	99	99
IOL (%)	41	44	46	50	62	65	70	91	98	103
RR	3.21	3.16	1.25	1.07	0.52	0.99	0.18	0.12	0.18	0.15

Table 4. Evolution of hydrolysis phenomenon of profile KY1

Pedological level	Samples	Lithology	SiO_2/Al_2O_3	Hydrolysis process	Minerals
	P10	Md	0.15		Gibbsite,
	P9	Md	0.18	allitisation	Goethite, Hematite and other Fe-oxides
alloterite	P8	Pd	0.12		
	p7	Pd	0.18		
	P6	Nd	0.99		
	P5	Sc	0.52		
isalterite	P4	Fs	1.07		Halloysite/Metahalloyiste
	P3	Cs	1.25	monosiallitisation	Kaolinite,
Weathered	P2	Bw	3.16		Smectite
Parent rock	P1	B	3.21	bisialitisation	(montmorillonite)

B=basalt; Wb=weathered basalt; Cs=coarse saprolite; Fs=Fine saprolite; Sc=Spoted clays; Md=massive duricrust; Pd=Pisolitic duricrust, Nd=nodular duricrust; R=redish; Br=brown red; Md=massive duricrust; Pd=Pisolitic duricrust, Nd=nodular duricrust

3.3.5 Rare Earth Element (RRE) and fractionation

The rare earth elements are mobile during the formation of soil [37-41]. In the Bangam weathered mantle, the results are represented in Table 2: The light rare earth elements (LREE) are more dominant with Ce (27.8ppm - 552ppm), La (40.5ppm - 121ppm) and Nd (11.9ppm - 90.9ppm); the heavy rare earth elements (HREE) which are poorly represented here by Lu (0.18ppm - 0.44ppm), Yb (1.27ppm - 3.58ppm), and is particularly marked by a high content of Y (6.6ppm - 103.5ppm).its confirms by the ratio ∑LREE/∑HREE (4.26 - 14.18) in Table 2. The chondrite and basalt -normalized (Fig. 6) patterns confirm an important enrichment of LREE and an impoverishment of HREE along of profile as others lateritic soils. We also observe according the basalt normalized patterns, a positive anomaly in Ce and Yb, a negative anomaly in Ce, Dy and Tm. In addition, chondrite normalized also shows negative anomaly in Ce, Eu and Ho, a positive anomaly in Ce and Eu. The Eu/Eu* ratio, related to the REE fractionation, varies from 0.38 to 1.13, indicating important fractionation of the REE in various lateritic soil phases, with weak negative Eu anomaly. The Ce/Ce* ratio, included between 0.59 to 1.08 show a positive anomaly of Ce in the coarse saprolite and negative anomaly in the bauxite duricrust. The (La/Yb)N ratio, which ranges from 0.7 to 8.83, also indicates a strong fractionation of the LREE compared to the HREE.

4. DISCUSSION AND INTERPRETATION

4.1 Chemical Evolution in the Weathering Mantle

The phenomenon of weathering mantel have been studied by many author's such as [42-47] and the better method to understand weathering mantle in this case of Bangam profile is by using chemicals alteration index to appreciate it. The weathering mantle is organized in three levels link by a morphogenesis, according to the texture and structure, the upper domain or alloterite of alteration coat is dominated by a complete transformation of primary minerals and a great blocs of bauxite duricrust, the RR or molar ratio SiO_2/Al_2O_3 as indicated in Table 3 is very low [48] and a strong CIA translate a high leaching of clay particles in this part of profile and the formation of the gibbsite, goethite, hematite and others iron hydroxides. In the isaltérite, the weathering index are moderate and less than in the allotérite, it's dominated by mottled clays, this

environment indicate an alkaline environment [46] responsable of the formation of kaolinite and others 1/1 minerals such as halloyisite and metahalloysite suitable for specific hydrolysis known as monosialitisation [48-50]. The progression towards the base of profile leads to

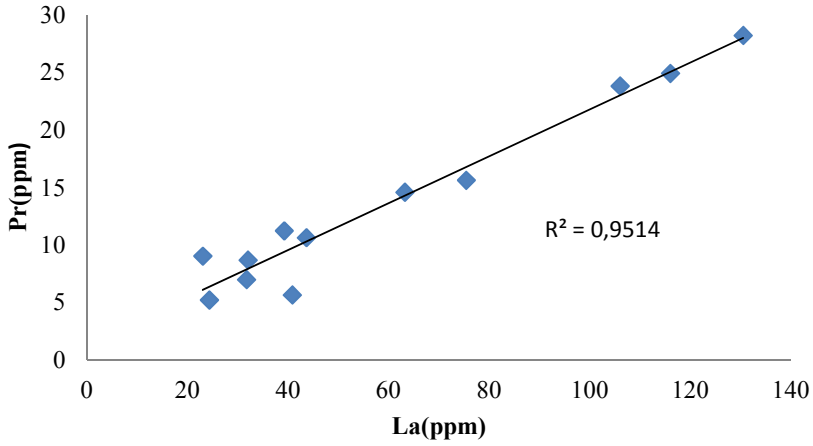

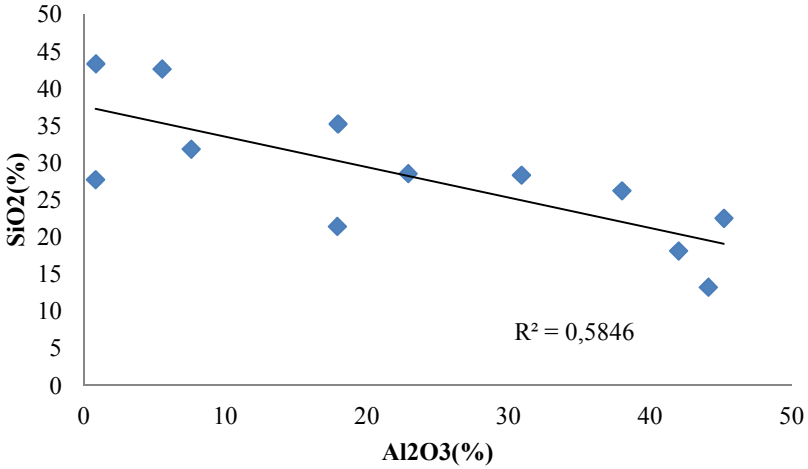

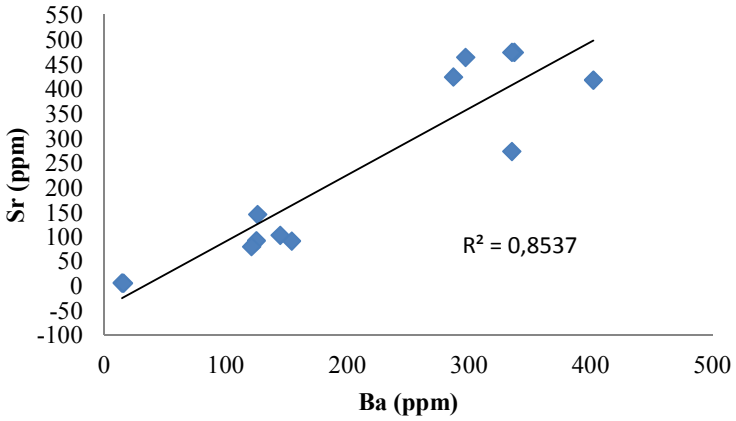

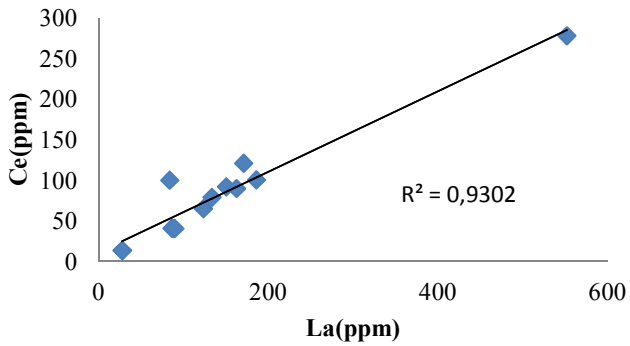

Fig. 6. Binary plots of selected major elements (wt %) and trace and REE elements (ppm) R= correlation

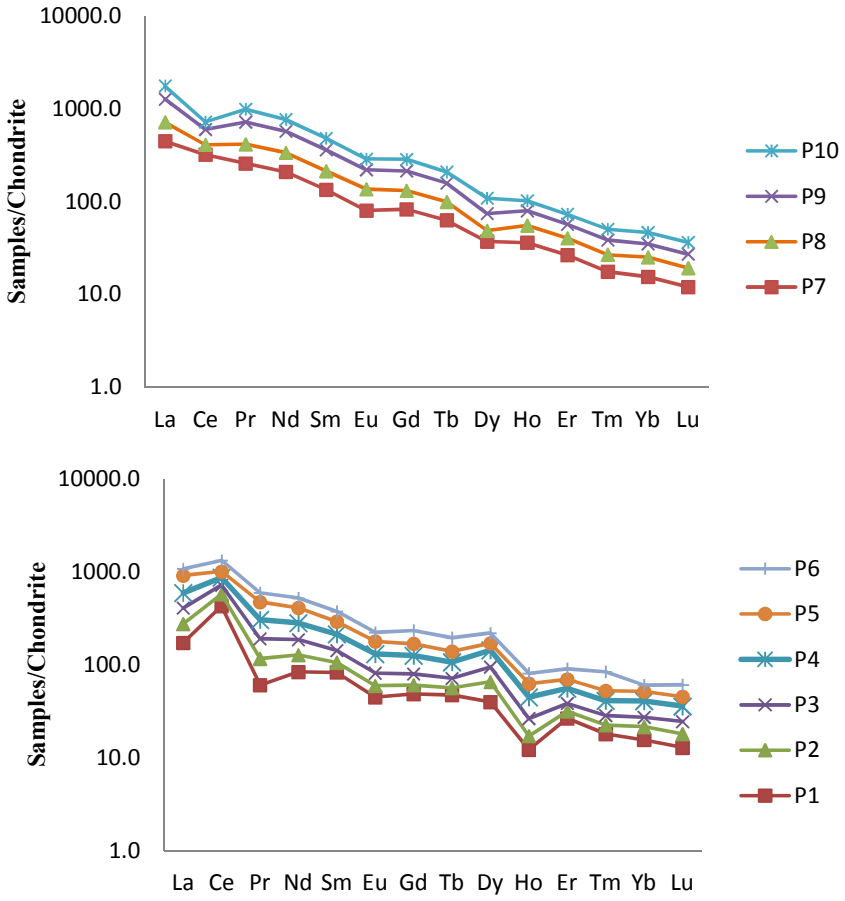

Fig. 7a. Samples/ Chondrite-normalized REE patterns in the weathering KY1 profile

the primary minerals. In the other hand, the base of profile is also characterized by a low porosity, a relics of bedrock, a fine grain particles and "pain epice"clays, the RR is strong and CIA is low at the base of profile just indicate the presence of 2/1 clays minerals of smectites

group [51,52] such as montmorillonite because of the weak leaching or high contents of Mg, K and Si in this part of the profile [53], these environments are indicative of a highly confined alkaline environment suitable for hydrolysis known as bisialitisation. The data in the Table 4 and Fig. 3 might confirms the hypothesis of an in situ model according to [48] and [54] where the lithomarge is developed on a basaltic rock. The isaltéritique level which or intermediate between alloterite and weathered basalt is the domain where the simultaneous hydrolysis phenomena favorable to the genesis of clays 2/1 and 1/1 completing the uncertain hypothesis of [8] on the genesis of Bangam bauxites. The antagonism between the RR and CIA as we observe in this case of Bangam KY1 profile is the logic symbol of the chemical elements manifestation in the lateritic zone.

4.2 Petrographical and REE Evolution in the Weathering Mantle

Occurrences of bauxite as a result of the weathering of basalt are reported in Madagascar [55] and in the South-Cameroon [56] on the syenite weathered mantle. These Bangam bauxite deposits are clearly considered as formed by direct bauxitization process, resulting from initial primary rock. The development of secondary minerals as gibbsite kaolinite goethite hematite and other, petrographically, these supergene minerals were reported as pseudomorphs after primary minerals such as olivine, pyroxenes, plagioclases and magnetite, the replacement was considered isovolumetric as defined by [57]. Therefore, the origin of montmorillonite or some minerals of smectite group was successively investigated in the alteration of plagioclases and pyroxenes respectively by [58,59,60]. Although the first stage of parent minerals weathering generate segregations and spots of iron oxyhydroxides aren't observed in Fig. 2, iron accumulation is really developed in and can be derive from the alteration of olivine or other ferromagnesian minerals. The first stage of the alteration of plagioclases was classically explained by [55] and [61], it can generate a primary gibbsite and metahalloysite present in "pain d'epice" (greyish section) of first stage of the alteration of basalt. The gain and loss of chemical elements as we observe the balance mass and the distribution translate the relative and absolute accumulation of major, trace and REE along the Bangam profile according to [62]. KY1 Bangam profile shows that during alteration process, the leaching and mobility of some chemical elements such as Na^{+}, Ca^{2+}, K^{+}, Mg^{2+}, Mn^{2+}, Si^{4+} are proportional to the degree of weathering [63]. These elements are preferably leached [28]. Whereas Al^{3+}, $Fe^{3+}$and Ti^{4+} are more often constant in the weathering system [64-67]. The bauxitisation process is explained by the ternary diagrams of IOL and CIA, it's indicated a domination by alumina and iron phases (see Fig. 8). The transformation of primary minerals as we observe in thin section, shows a progressive changing from greyish color, rich in 2/1 minerals to a whitish-grey, rich in kaolinite and finally whitish, rich in gibbsite. This observation in the thin sections is nothing other than the reflection of the phenomenon that took place in the weathering mantle according to the classification of Table 4 based on the molar ratio SiO_2/Al_2O_3 or Ruxton ratio adopted by [51,52,49]. The antagonism process of lateritic phase, between aluminous minerals such as gibbsite, kaolinite and ferruginous minerals such as goethite and hematite along the weathered zone prove a correlation of chemical elements; an evidence of a genetic link of different horizon (see Fig. 6) such observed SiO_2-Al_2O_3 and Sr-Ba and others REE isochrons. During the formation of soil, the mobility and structural reorganization of REE involve automatically their fractionation [38-41] and consequently the features of the parent rock remain along the Bangam KY1 profile favoured by the circulation of meteorite waters or the pH/Eh of environment. The Chondrite and basalt -normalized REE indicates a light rare earth enrichment (LREE) relative to heavy rare earths (HREE) due to higher stability of the ligands (sulphates and carbonates) and higher redistribution along the profiles during lateritic alteration [68-74] and [39], the mobilization of the REE during weathering processes results from different factors related to the parent rock mineralogy, specifically the distribution of the REE in the primary bearing minerals, the stability of these minerals during weathering, and their abundance in the parent material. In addition, the low values of (La/Yb) N (0.79-8.83), may be attributed to intense REE fractionation [75]. The chondrites /samples and basalt/samples normalized patterns (Figs. 7a and 7b) reflect a unique source of samples collected in the alteration zone [76] and similar epigenetic transformations for basaltic rocks such as most lateritic profiles [77]. A light negative anomaly in Ce is due to the oxidation-reduction conditions [78] and its incorporation into the ferromanganese-ferric module in the form of ceric oxides or insoluble cerianite [79-81]. [79]

also suggest that, negative anomaly in Ce is due of the formation of new minerals especially the montmorillonite. Cerium can occur in the nature as Ce^{3+} in reducing conditions like the majority of

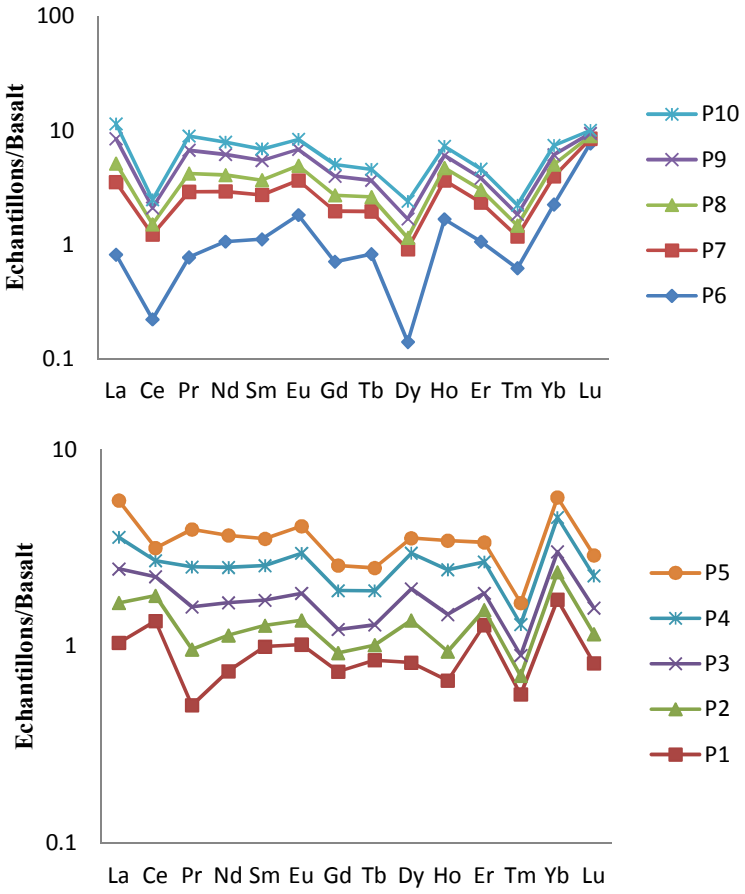

Fig. 7b. Samples/ Basalt-normalized REE patterns in the weathering profile

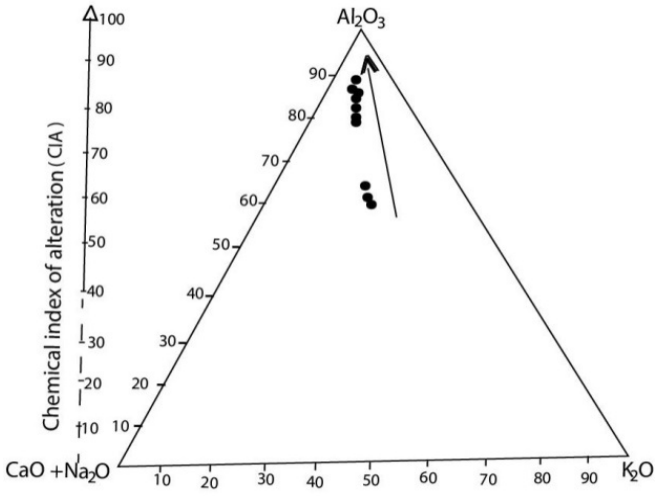

Fig. 8a. Al_2O_3–K_2O–CaO +Na_2O (wt%) ternary diagram for the Bangam lateritic profile(KY1).The evolution of feldspars and primary minerals based on Nesbitt and Young (1982)

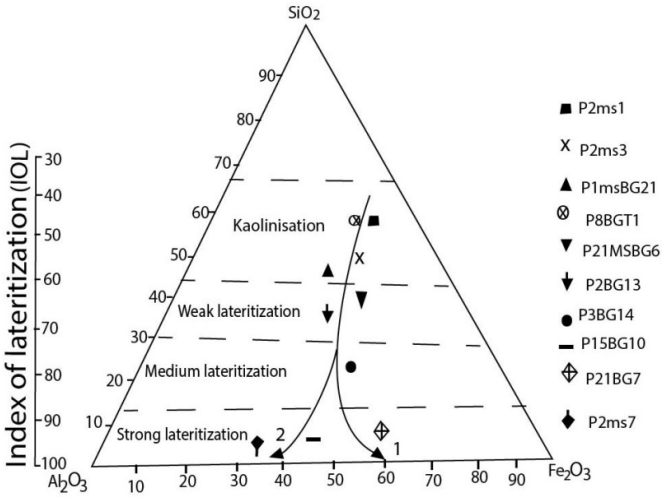

Fig. 8b. Al_2O_3–SiO_2–Fe_2O_3(wt%) ternary diagram for the Bangam lateritic profile(KY1).The fields of kaolisation, weak, medium and strong lateritization, based on Babechuk et al. (2014)

lanthanides. Or as Ce^{4+} in oxidizing conditions. If soluble Ce^{3+} is oxidized to Ce^{4+}, it precipitates from solution as very insoluble CeO_2 or according to [82], Cerium and others lanthanides (Yb, Ho, Dy, Eu…) have a particular fractionation because of their multiple ionic valences. The positive and negative anomaly in the Bangam profile behaviors is due by the moving of phreatic sheet in the alteration weathering which would be responsible for rare earth leaching (Figs. 7a & 7b). In the other hand, alteration coat shows a negative Cerium anomaly may be linked to oxidation of Ce^{3+} to Ce^{4+} or primary Ce^{4+} in residual zircon or sphene minerals because of it's oxidation ability, insolubility and stability in lateritic environments [18].

5. CONCLUSION

The weathered profile is dominated by an evolution of alumina and iron phases and the gibbsite observed is primary and secondary minerals.

The mechanism of bauxitisation along the weathering mantle of the Bangam locality shows that the chemical evolution respects to the law of lateritization in tropical environment. The bauxitisation process started by the weathering of basalt, characterized by an alternate domain rich in Al_2O_3 and Fe_2O_3 commonly research by the mining company.

The geochemical continuity between the three major levels of alteration confirms that the Bangam bauxites are autochthonous. The bauxitisation process has been strongly influenced by the pH, temperature and the nature of parent rock. The process of bauxitisation has undergone a normal evolution from bisialitisation, monosiallitisation to allitisation. In the other words, the different samples are cogenetic, which are formed at the same time, in the same parent rock known as basalt. Since the first tertiary volcanic phase that affected the region of Western Cameroon.

COMPETING INTERESTS

Authors have declared that no competing interests exist.

REFERENCES

1. Dongmo JL. Les dynamismes Bamilékés. Tomes I, la maitrise de l'espace agraire, Yaoundé CEPER. 1981;424.
2. Melingui A, Gwanfogbe M, Ngoughia J. Géographie du Cameroun. Edition CEPER. Yaounde. 1989;119.
3. Letouzey R. Etude phytogéographique du Cameroun. Édition. p.Lechevelier; 511.
4. Deruelle B. Risque volcanique au Mont-Cameroun. Rev. Geo. Cameroon. 1982;3(1):33-40.
5. Fozing EM. Etude des amphibolites et des mylonites du Massif de Fomopéa. Thèse de Master, Université de Dschang. 2009;88.

6. Talla V. Le massif granitique panafricain de Batié (Ouest- Cameroun): Pétrologie pétro structurale- géochimie. Thèse Doctorat 3eme Cycle. Univ. de Yaoundé. 1995;144.
7. Kwékam M. Genèse et évolution des granitoïdes calco-alcalin au cours de la tectonique panafricaine: le cas des massifs syn à tardi- tectoniques de l'ouest-cameroun (région de Dschang et Kékem). Thèse d'Etat, Université de Yaoundé I. 2005;175.
8. Hiéronymus B. Etude minéralogique et géochimique des formations bauxitiques de l'Ouest Cameroun. Collection ORSTOM. 1972;77-112.
9. Hiéronymus B. Etude de l'altération des roches éruptive de l'Ouest Cameroun. Unpublished Doctorat ès sciences.Thésis University Paris VIieme; 1985.
10. Tardy Y. Petrology of laterites and tropical soils. Balkema, Amsterdam, The Netherlands. 1997;459.
11. Bilong P, Eno Belinga SM, Volkoff B. Séquence d'évolution des paysages cuirassés et des sols ferrallitiques en zone forestière tropicale d'Afrique Centrale. Place des sols à horizon d'argile tachetée. Comptes Rendus de l'Académie des Sciences, Paris, France. 1992;314(2):109–115.
12. Aleva G. J. J. Laterites. Concepts, geology, morphology and chemistry. Wageningen: ISRIC. 1994;169.
13. Temgoua E, Bitom D, Bilong P, Lucas Y, Pfeifer HR. Démantèlement des paysages cuirassés anciens en zone forestière tropicale d'Afrique Centrale, formation d'accumulations ferrugineuses actuelles au bas des versants. Comptes Rendus Géoscience. 2002;334:537–543.
14. Bitom D, Volkoff B, Abossolo, Angue M. Evolution and alteration *in situ* of a massive iron duricrust in Central Africa. Journal of African Earth Sciences. 2003;37:89–101.
15. Bitom D, Volkoff B, Beauvais A, Seyler F, Ndjigui PD. Rôle des héritages latéritiques et du niveau des nappes dans l'évolution des modelés et des sols en zone intertropicale forestière humide. Comptes. Comptes Rendus Géoscience. 2004;336:1161–1170.
16. Eno, Belinga SM. Altération des roches basaltiques et processus de bauxitisation de l'Adamaoua. Thèse de Doctorat d'Etat, Univ. de Paris V ieme. 1972;570.
17. Momo NM. Les surfaces latéritiques cuirassées du plateau Bamiléké (Ouest-Cameroun): Cartographie du potentiel bauxitique, pétrologie, contexte morpho-tectonique et dynamique du paysage. Thèse de doctorat/PhD. Univ. Dschang. 2016;223.
18. Ndjigui PD, Bilong P, Bitom D, Dia A. Mobilization and redistribution of major and trace elements in two weathering profiles developed on serpentinites in the Lomie´ ultramafic complex, South-East Cameroon. Journal of African Earth Sciences. 2008;50:305–328.
19. Nguetnkam JP, Kamga R, Villiéras F, Ekodeck GE, Yvon J. Altération différentielle du granite en zone tropicale. Exemple de deux séquences étudiées au Cameroun (Afrique Centrale). Comptes Rendus Géoscience. 2008;340:451–461.
20. Kamgang KBV, Onana VL, Ndome EPE, Parisot JC, Ekodeck GE. Behaviour REE and mass balance calculations in a lateritic profile over chlorite schists in South Cameroon. Chemie der Erde-Geochemistry. 2009;69:61–73.
21. Tsozué D, Bitom D, Yongue FR. Morphology, mineralogy and geochemistry of a lateritic soil sequence developed on micaschist in the Abong-Mbang region, Southeast Cameroon. South African Journal of Geology. 2012;115(1):103-116.
22. Ndjigui PD, Badinane MFB, Nyeck B, Nandjip HPK, Bilong P. Mineralogical and geochemical features of the coarse saprolite developed on orthogneiss in the SW of Yaoundé, South Cameroon. Journal of African Earth Sciences. 2013;79:125–142.
23. Hieronymus B. Bauxites latéritiques et bauxites: Cas du contact forêt-savane du Sud-Est Cameroun. Thèse d'État, Université de Yaoundé-1. 1973;208
24. Sojien MT. Etude petrographique, mineralogique et geochimique des formations bauxitiques de Bangam dans les Hautes terres de l'Ouest Cameroun. Mémoire de MSc. Université Dschang, Dschang. 2007;77.
25. Momo NM, Tematio P, Yemefack M. Multi-scale organization of the Doumbouo-Fokoué Bauxites Ore Deposits (West Cameroon): Implication to the landscape lowering. Open Journal of Geology. 2012;14-24.
26. Sojien TM, Mamdem TEL, Wouatong ASL, Bitom DL. Mineralogical and geochemical

distribution study of bauxites in the locality of bangam and environs (West Cameroon). Earth Science Research. 2017;7(1). ISSN: 1927-0542. E-ISSN: 1927-0550. Published by Canadian Center of Science and Education.

27. Maignien R. Manuel de prospection pedologique.Doc ORSTOM. Manuel sur les routes dans les zones tropicales et desertiques. Tome 2.étude technique de construction. 1968;244-277. BCEOM-CEBTP; 1991.
28. Nesbitt HW, Young GM. Early proterozoic climates and plate motions inferred from major element chemistry of lutites. Nature. 1982;199:715-717.
29. Ruxton BP. Measures of the degree of chemical weathering of rocks. Journal of Geology. 1968;76.
30. Babechuk MG, Widdowson M, Kamber BS. Quantifying chemical intensity and trace element release from two contrasting profiles. Decan Traps, India Chemical Geology. 2014;365:56-75.
31. Malpas J, Duzgorem-Aydin NS, Aydin A. Behaviour of chemical elements during weathering of pyroclastic rocks, Hong-Kong. Environment International. 2001;26:359-368.
32. Anders E, Grevesse N. Abundances of the elements: Meteoritic and solar. Geochimica and Cosmochimica Acta. 1989;53(1):197-214.
33. Taylor SR, Mc Lennan SM. The continental crust: Its composition and evolution. Blackwell, Oxford. 1985;321.
34. Delvigne J. Micromorphology of mineral alteration and weathering. The Canadian Mineralogist 3, ORSTOM éd. 1998;494.
35. Biton D. Organisation et évolution d'une couverture ferralitique en zone tropicale humide (Cameroun). Genèse et transformation d'ensemble ferrugineux indurés profonds. Thèse. Univ. Poitiers. Multigr. 1988;164.
36. Moinereau J. Altération des roches, formation et évolution des sols sur basalte. Sous climat tempéré humide. Thèse de Doct. d'Etat. Univ. des Sci. et Tech. du Languedouc. 1977;197.
37. Nesbitt HW. Mobility and fractionation of rare earth elements during weathering of granodiorite. Nature. 1979;279:206-210. DOI: 10.1038/279206a0
38. Duddy R. Redistribution and fractionation of rare earth and other elements in a weathering profile. Chem. Geol. 1980;30:363-381.
39. Humphris SE. The mobility of the rare earth elements in the crust. In Rare Earth Element Geochemistry (éd. P. Henderson) Elsevier. 1984;Chap. 9:317-340.
40. Middelburg JJ, Van Der Weijden CH, Woittiez JRW. Chemical processes affecting the mobility of major, minor and trace elements during weathering of granitic rocks. Chem. Geol. 1988;68:253-273.
41. Mc Lennan SM. Rare earth elements in sedimentary rocks: Influence of provenance and sedimentary processes. In Geochemistry and mineralogy of rare earth elements. (éd. Lipin B. R. & McKay G. A.), Reviews in Mineralogy. 1989;21:169-196.
42. Trescases JJ. L'évolution géochimique supergenes des roches ultrabasiques en zone tropicale. Formation des gisements nickélifères de Nouvelle-Calédonie: Mém. ORSTOM. 1975;78:259.
43. Edou, Minko A. Pétrologie et géochimie des latérites à ''stoneline'' du gîte d'or d'Ovala - Application à la prospection en zone équatoriale humide (Gabon). Th. Doc., Univ. de Poitiers. 1988;147.
44. Ouangrawa M, Trescases JJ, Ambrosi JP. Evolution des oxydes de fer au cours de l'altération de roches ultrabasiques de Nouvelle Calédonie: C.R. Acad. Paris, 323. 1996;lia:243-249.
45. Ndjigui PD. Métallogénie de la serpentinite de Kondong I et de son manteau d'altération dans le Sud-Est du Cameroun: Pétrographie, minéralogie et géochimie. Th. Doc. 3e Cycle, Univ. Yaoundé I. 2000;170.
46. Ndjigui PD, Bitom D, Bilong P, Colin F, Ali HN. Correlation between metallic oxides (Fe_2O_3, Cr_2O_3, NiO) platinum and palladium in the laterites from Southeast Cameroon (Central Africa). Perspectives of Platinoids Survey in Weathering Mantles, 9th International Platinum Symposium. Abs. Duke University; 2002.
47. Ekodeck GE. L'altération des roches métamorphiques du sud Cameroun et ses aspects géotechniques. Th. Doct. Etat es sci. Nat., IRGM, Univ. Scientif. Et Médic. De Grenoble I – France. 1984;368.
48. Nahon D. Cuirasses ferrugineuses et encroutements calcaires au Sénégal oriental et en Mauritanie. Systèmes évolutifs: géochimie, structures, relais et

coexistence. Mém. Sci. Géol. 1976;44:232,12 pl. h.t.
49. Beauvais A. Ferricrete biochemical degradation on the rainforest savannas boundary of Central African Republic. Geoderma. 2009;1(50):379–388.
50. Zobir HS. Impact de l'altération sur le bilan chimique des diatexites du Massif de l'Edough (Annaba, NE Algérien) Estudios Geológicos. 2012;68(2):203-215. ISSN: 0367-0449.
DOI: 10.3989/egeol.40612.158
51. Millot G. Géologie des argiles. Masson et Cie, éd.: Paris. 1964;499.
52. Tardy Y. Géochimie des altérations. Étude des arènes et des eaux de quelques massifs cristallins d'Europe et d'Afrique. Thèse de Doctorat d'État, Université Strasbourg, Mémoires du Service de la Carte géologique. Alsace-Lorraine. 1969;31:199.
53. Tematio P, Kombou NA, Kengni L, Nguetnkam JP, Kamgang KV. Mineral and geochemical characterization of the weathering mantle derived from norites in Kekem (West-Cameroon): Evaluation of the related mineralization. International Research Journal of Geology and Mining (IRJGM), (2276-6618). 2012;2(8):230-242.
54. Leprun JC. les cuirasses ferrugineux des pays cristallins de l'Afrique occidental seche.Genese-transformation-degradation. Mem. Sci Géologique. 1979;58:224.
55. Gense C. Altération du basalte dans une basse-colline de la côte-Est de Madagascar (unité morphologique de cette région) Cahier. ORSTOM, sér. Géol.II. 1970;2:249-258.
56. Bilong P. Genèse et développement des sols ferrallitiques sur syenite alcaline potassique en environment forestier du centre-sud Cameroun. Comparaison avec les sols ferrallitiques développés sur roches basiques. Ph.D. Dissertation. University of Yaoundé Cameroun; 1988.
57. Millot G, Bonifas M. Transformations isovolumétriques dans les phénomènes de latéritisation et de bauxitisation. Bull. Serv. Carte Géol. Alsace. Lorraine. 1955;8:3-10.
58. Nguetnkam JP, Bitom D, Yongue R, Bilong P, Belinga ESM, Volkoff B. Etude pétrologie, minéralogique et géochimique d'une toposéquence de sols développés sur granite dans le plateau forestier Sud-Camerounais. Sciences, Technique et Développement. 2003;10:35-43.
59. Craig DC, Loughnanf C. Chemical and mineralogical transformation accompanying the weathering of basic volcanic rocks from New South Wales. Aust. J. Soi/.Res. 1964;2:218-234.
60. Loughnan JC. Chemical weathering of the silicate minerals. Am. Elsevier Publ. Comp. I'nc. New York. 1969;146.
61. Bates TF. Halloysite and gibbsite formation in Hawaï. Proc. Nat. Conf. Clays and Clays Minerals, 9:307-314. Rendus de l'Académie des Sciences, Paris, France. 1962;314(2):109–115. Rendus Géoscience. 336:1161–1170.
62. D'Hoore J. Accumulation des sesquioxydes libres dans les sols tropicaux. I.N.E.A.C. 1954;62:131.
63. Wronkiewicz DJ, Condie KC. Geochemistry of Archean shales from the Witwatersrand supergroup, South Africa: Source-area weathering and provenance. Geochimica et Cosmochimca Acta. 1987;51:2401-2416.
DOI: 10.1016/0016-7037 (87) 90293-6
64. Gresens RL. Composition-volume relationships of metasomatism. Chemical Geology. 1967;2:47-65.
DOI: 10.1016/0009-2541 (67) 90004-6
65. Grant JA. The isochron diagram – a simple solution of Gresens' equation for metasomatic alteration. Economic Geology. 1986;81:1976-1982.
DOI: 10.2113/gsecongeo.81.8.1976
66. Potdevin JL, Caron JM. Transferts de matière et déformation synmétamorphique pli. I: Structureset bilans de matière. Bulletin de Mineralogie. 1986;109(4):395-410.
67. Potdevin JL, Marquer D. Méthodes de quantification des transferts de matière fluides dans les roches métamorphiques déformées. Geodinamica. 1987;Acta1(3):193-206.
68. Steinberg M, Courtois C. Le comportement des terres rares au cours de l'altération et ses conséquences. Bull. Soc. Geol. France. 1976;1:13-20.
69. Topp SE, Salbu B, Roaldset E, Jorgensen P. Vertical distribution of trace elements in laterite soil (Suriname). Chem. Geol. 1984;47:159-174.
70. Trescases JJ, Fortin P, Melfi A, Nahon D. Rare earth elements accumulation in lateritic weathering of Pliocene sediments, Curitiba Basin (Brazil). In Proceeding of the International Meeting Geochemistry of

the Earth Surface and Process of Mineral Formation. Grenade. 1986;260-271.
71. Fortin P. Mobilisation, fractionnement et accumulation des terres rares lors de l'altération latéritique de sédiments argilo-sableux du bassin de Curitiba (Brésil). Thèse. Mém. Sci. de la Terre n01O, ENSMP. 1986;186.
72. Marker A, D'Oliveira JJ. The formation of rare earth element scavenger minerals in weathering products derived from alkaline rocks in SE-Bahia, Brazil. (Abs.). Chem. Geol. 1990;84:373-374.
73. Melfi AJ, Figueiredo AM, Kronberg B, Dohert WD, Marques LS. REE mobilities during incipient weathering of volcanic rocks of the Parana Basin, Brazil. (Abs.). Chem. Geol. 1990;84:375-376.
74. Soubies F, Melfi AJ, Autefage F. Geochemical behavior of rare earth elements in aiterites of phosphate and titanium ore deposits in Tapira (Minas Gerais, Brazil): The importance of phosphates. Chem. Geol. 1990;84:376-377.
75. Moroni M, Girardi VAV, Ferrario A. The Serra Pelada Au-PGE deposit, Serra dos Carajas (Para State, Brazil): Geological and geochemical indications for a composite mineralising process. Mineral Deposita. 2001;36:768–785.
76. Sun S, McDonough WF. Chemical and isotopic systematics of oceanic basalts; implications for mantle composition and processes. In: Magmatism in the Ocean Basins. (Saunders, A.D. & Norry, M.J. Eds.). Geological Society of London, London, United Kingdom. 1989;313-345.
77. Ronov AB, Balashov YA, Migdisov AA. Geochemistry of the rare earths in the sedimentary cycle. Geochem. Inti. 1967;4:1-17.
78. Goldberg ED. Chemistry in the oceans. In Oceanography (éd. M. Shears). Am. Assoc. Adv. Sei. 1961;Pub. 67:583-597.
79. Piper DZ. Rare earth elements in ferromanganese nodules and other marine phases. Geochim. Cosmochim. Acta. 1974;29:1007-1022.
80. Michard G, Renard D. Possibilités d'entraînement du cobalt, du plomb et du cérium dans les nodules de manganèse par oxydation. C. R. Acad. Sc. Paris. 1975;280:1761-1764.
81. Tlig S. Distribution des terres rares dans les fractions de sédiments et nodules de Fe et Mn associés en l'Océan Indien. Mar. Geol. 1982;50:257-274.
82. Braun JJ, Maurice P, Muller JP, Bilong P, Michard A, Guillet B. Cerium anomalies in lateritic profiles. Geochimica el Cusmochimica Acta. 1989;54:781-795.

Peer-review history:
The peer review history for this paper can be accessed here:
http://www.sdiarticle3.com/review-history/49572